Intrinsic and Environmental Effects on the Kinetic and Thermodynamics of Linkage Isomerization in Nitritopentaamminecobalt(III) Complex

Ilaria Ciofini

Institut de Chimie Inorganique et Analytique, Université de Fribourg Pérolles, CH-1700 Fribourg, Switzerland

Carlo Adamo*

Laboratoire d'Electrochimie et de Chimie Analytique, UMR 7575, E.N.S.C.P., 11 rue P. et M. Curie, F-75231 Paris Cedex 05, France

Received: September 28, 2000; In Final Form: November 15, 2000

In this paper we present a theoretical study of the linkage isomerization in $[Co(NH_3)_5ONO]^{2+}$. In particular, we have used for our analysis a hybrid density functional/Hartree−Fock method for the electronic computations (the so-called B3LYP), while a recent version of the polarizable continuum model has been considered to model solute−solvent interactions. A particular effort has been devoted to understand the kinetics of the reaction and to assess the nature of the transition state. Our results show that this reaction is only marginally exothermic in the gas phase, while solvent significantly shifts the equilibrium toward the nitro isomer. We have also identified the transition state of the reaction, which can be described as a heptacoordinate structure with the NO_2 group in η_2 coordination.

1. Introduction

The fast isomerization of nitrite ion bound to pentaamminecobalt(III) complex is the first known example of linkage isomerism in coordination chemistry.[1−3] This reaction has been so extensively studied by experimentalists that it is now considered in all inorganic chemistry textbooks as the prototype of this class of reactions.[4,5] Furthermore, a number of similar complexes, characterized by different metal centers and ligands, undergo a similar isomerization.[6−9] The kinetics and the thermodynamics of the spontaneous isomerization of the nitritopentaamminecobalt(III) complex, $[Co(NH_3)_5ONO]^{2+}$, in the corresponding nitro complex, $[Co(NH_3)_5\ NO_2]^{2+}$, have been studied both in solution and in the solid state.[10−17] This reaction was proved to be intramolecular by using different experimental techniques. In fact, the kinetics in aqueous solution is independent of the NO_2^- concentration added[11] and ^{18}O tracer techniques showed that neither the inner Co−O or the outer NO oxygen of the nitrito complexes exchange with solvent during the isomerization.[10] Also, activation volumes for isomerization are consistent with an intramolecular mechanism.[13] A similar intramolecular mechanism has been postulated in the solid state.[14]

These results clearly establish that the nitrite ion never leaves the influence of the coordination sphere but they do not give any strong indication about the nature of the transition state. Three activated complexes consistent with the intramolecularity of the process have been envisaged (see Scheme 1): a heptacoordinate state (I) (η_2 coordination), a pentacoordinate tight ion pair (II), or a six-coordinate π-bonded species (III) (η_3 coordination).

When the reaction is carried out in a solvent that readily dissociates ion pairs, yet no exchange is detected. Also, high ionic strength of the media does not promote the dissociation of the ion-paired species.[8] As a consequence, the ion-pair (structure II) appears to fit the experimental observations least and has been discarded by the same experimentalists.[8]

SCHEME 1

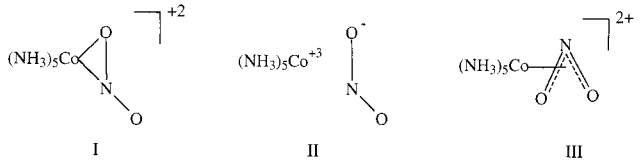

I II III

More involved is the situation for the other two possible structures. In fact, from one side the evaluated transition state volume is consistent with the intermediate type envisaged by Basolo and Pearson[11] (structure I), while from the other, ^{17}O NMR data are more consistent with a η^3 coordination (structure III).[17] Unfortunately, the experimental data do not allow for a deeper understanding of reaction mechanisms, so that the question concerning the nature of the transition state is still unanswered.

In such circumstances, quantum mechanical approaches can offer a valuable support to the experiments in choosing between the concurrent interpretations of the reaction mechanism. Furthermore, theoretical methods allow for an easy evaluation of the contribution of different terms to the overall result, tunable by switching *on* and *off* the different interactions in the computations. Of course, the computational protocol must provide reliable structural and thermochemical data, two requirements which are not always straightforward to obtain for organometallic complexes.[18]

Density functional theory (DFT) has been remarkably successful in providing means for computing a variety of properties for organometallic compounds with a good accuracy.[19] In particular, the so-called hybrid density functional/ Hartree−Fock methods, where some Hartree−Fock (HF) exchange is added to the DFT contributions,[20] provide deep insight in the electronic

* Corresponding author. E-mail: adamo@ext.jussieu.fr.

10.1021/jp003551k CCC: $20.00
Published on Web 01/20/2001

structure of transition metal complexes and their reactivity.[21−26] Anyway, the availability of an accurate computational electronic tool is not enough, since most reactions take place in solution, and a complete theoretical analysis must include a proper treatment of the solute−solvent interactions. In this context, solvent models rooted in the polarizable continuum approach[27] are particularly appealing for the evaluation of solvent shifts on physicochemical properties of chemical systems. While the procedure is well attested for organic molecule and reactions (see for instance refs 28 and 29), only a few applications have been done in the field of organometallic chemistry.[30,31]

On this basis, we decided to focus our attention on the thermodynamics and the kinetics of linkage isomerization in the nitritopentaamminecobalt(III) complex, with the double aim of elucidating the reaction mechanism of the linkage isomerization and showing the flexibility of the proposed computational tool in the field of the organometallic chemistry.

2. Computational Details

Density functional calculations were carried out within the Kohn−Sham (KS) formalism, as implemented in the developing version of the Gaussian code.[32] In particular, we have chosen the so-called B3LYP model, a self-consistent hybrid approach[33] obtained by a combination of HF and Becke exchange[34] with the Lee, Yang, and Parr correlation functional.[35] All the molecular structures have been fully optimized both in the gas phase and in solution using the quasi-relativistic effective core potentials (ECP's) of Hay-Wadt[36] for cobalt. The double-ζ quality basis set of Huzinaga and Dunning was, instead, considered for all the other atoms.[37] This ECP and the chosen basis sets will be referred in the following as LANL2DZ.

The combined use of the B3LYP approach with this ECP has been tested and validated in a number of studies on organometallic complexes and reactions.[24,25,38,39,40] Single-point energy evaluations have been carried out at the optimized geometries adding one d polarization function on N and O (exp = 0.8 and exp = 0.85, respectively) and one p function on cobalt (exp = 0.14) (LANL2DZp).

Solvent effects were evaluated using a recent implementation of the polarizable continuum model (PCM) in the Gaussian package.[41,42] In particular, optimized structures, vibrational frequencies, and solvation energies have been computed by a cavity model, namely the united atoms topological model (UATM),[43] coupled to the new conductor-like polarizable continuum model (CPCM).[44] The details of this procedure have been extensively described elsewhere.[44−46] Here we simply recall that this approach provides results very close to those obtained by the original dielectric model for high dielectric constant solvents, but it is significantly more effective in geometry optimizations and frequencies calculations,[46] and less prone to numerical errors arising from the small part of the solute electron cloud lying outside the cavity (escaped charge effects).[45] Furthermore, it allows for an efficient analytical evaluation of the free energy second derivatives.[46]

All the stationary points found in the gas-phase or in aqueous solution, corresponding to reactant, transition state, and product, have been characterized by computing harmonic frequencies.

Finally, the electronic structure of these molecules either in the gas phase and in solution have been investigated using the natural bond orbital (NBO) approach and the related natural population analysis (NPA).[47] The NPA approach is particularly effective also for transition metal complexes, since it gives a description of the electronic distribution which is less sensitive to the computational parameters (e.g., basis set).[47] These computations have required the writing of a proper interface between the Gaussian package and the last public release (4.0) of the NBO program.[48] All the molecular structures have been obtained using the Molden graphical package.[49]

TABLE 1: Selected Bond Lengths (Å) and Valences Angles (deg) of the Two Isomers of Nitropentaamminecobalt(III) and the Transition State (TS) Structure[a]

	$[Co(NH_3)_5NO_2]^{2+}$		$[Co(NH_3)_5ONO]^{2+}$		TS
parameter	B3LYP	exp[b]	B3LYP	exp[c]	B3LYP
Co−N1	1.973	1.921 (19)	2.875		2.382
Co−N2	2.020	1.978 (19)	2.014	1.913 (8)	2.006
Co−N3	2.062	1.976 (16)	2.029	1.948 (4)	2.031
Co−N4	2.019	1.978 (19)	2.013	1.968 (9)	2.033
Co−N5	2.021	1.978 (19)	2.012	1.952 (4)	2.005
Co−N6	2.019	1.978 (19)	2.015	1.954 (4)	2.004
Co−O2	2.804		1.893	1.927 (5)	2.409
N1−O2	1.272	1.161 (22)	1.463	1.244 (9)	1.344
N1−O3	1.272	1.161 (22)	1.215	1.037 (10)	1.257
O2−N1−Co	117.7	123.0 (1)			
O2−N1−O3	124.4	113.9 (2)	112.5	125.3 (11)	118.3
Co−O2−N1			117.3	131.3 (9)	

[a] All values refer to the gas phase. [b] Reference 50. [c] Reference 14.

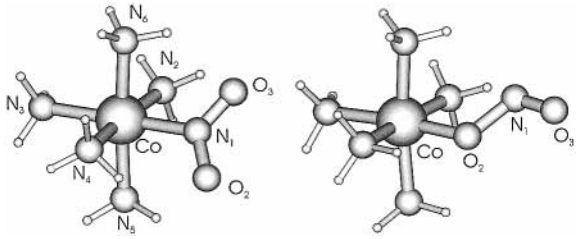

Figure 1. Structure and atom labeling of $[Co(NH_3)_5NO_2]^{2+}$ (left) and $[Co(NH_3)_5ONO]^{2+}$ (right) isomers.

3. Results and Discussion

3.1. Structures and Vibrational Frequencies. Even if the nitrito isomer is unstable and the interconversion to the corresponding nitro isomer is relatively fast, it has been prepared and isolated in the solid state and X-ray data are available.[14] These data, together with the corresponding values for the nitro complex[50] and our theoretical results, are collected in Table 1. The atom labeling is reported in Figure 1. The agreement between computed and experimental data is not good, the Co−NH_3 distances being systematically overestimated (up to 0.10 Å). An even greater discrepancy is found for the NO bond lengths, which are 0.10 Å too long with respect to the experimental values. This discrepancy between experience and theory might be ascribed to the crystal environment, where hydrogen bonds between different units and/or between one unit and the counterions significantly alter the molecular structure.[14] In fact, a better agreement for the Co−N bond lengths is found when the external electrostatic field generated by the solvent is taken into account. This field partially takes into account all the external perturbation of electrostatic origin, such as the electrostatic part of H-bond interactions and/or crystal packing effects.[27] Table 2 collects the geometrical parameters for the two isomers, obtained upon optimization (without any constrain) in three different solvents: tetrahydrofurano (THF), acetone, and water. These solvents are representative of different chemical environments and strengths of interaction, their dielectric constants going from 7.6 (THF), to 20.7 (acetone), to 78.4 (water).

In going from the gas phase to the solution, a general contraction of all the bond lengths is observed, proportional to

TABLE 2: Selected Bond Lengths (Å) and Valences Angles (deg) of the Two Isomers of Nitritopentaamminecobalt(III) and the Transition State (TS) Structure, Computed in Different Solvents

	$[Co(NH_3)_5NO_2]^{2+}$			$[Co(NH_3)_5ONO]^{2+}$			TS
parameter	THF	acetone	water	THF	acetone	water	water
Co−N1	1.961	1.966	1.964	2.831	2.860	2.829	2.487
Co−N2	1.992	1.989	1.981	1.990	1.984	1.979	1.991
Co−N3	2.010	2.003	1.986	1.993	1.987	1.972	1.948
Co−N4	1.991	1.990	1.979	1.986	1.989	1.973	1.978
Co−N5	1.992	1.994	1.980	1.986	1.986	1.974	1.986
Co−N6	1.995	1.991	1.981	1.989	1.985	1.978	1.986
Co−O2	2.812	2.817	2.827	1.912	1.920	1.929	2.509
N1−O2	1.279	1.280	1.283	1.400	1.395	1.372	1.336
N1−O3	1.279	1.280	1.283	1.239	1.241	1.254	1.269
O2−N1−Co	118.8	118.9	119.6				
O2−N1−O3	122.4	122.1	120.9	113.2	113.1	116.9	117.1

the magnitude of the solvent dielectric constant. This shortening (between 0.003 and 0.04 Å for the Co−N bond lengths in the two complexes) increases the agreement with the X-ray data. An even greater effect is found for the Co−N3 bond length which decreases of 0.08 Å in the nitro complex and 0.07 Å in the nitrito complex in aqueous solution. These geometrical variations are consistent with the stabilization of the charge separation structure (like $[Co(NH_3)_5]^{3+}\cdots NO_2^-$) in polar solvent. The net effect is the reduction of the donation from the nitro group to the pentaammine complex and the vanish of the trans effect in solution. This latter result is in full agreement with early kinetic studies[51] which reported the absence of any trans bond-weakening effect, and it has been noted also in the crystal structure.[14]

The other discrepancies between the experimental and computed geometrical parameters concern the NO_2 moiety in both isomers. Here, anyway, the precision of the X-ray data is questionable, since positional disorders lead to a very short (and in some case unreliable) N−O distance.[14]

Some insights on the electronic structures of such complexes can be obtained by looking at the NPA charges, calculated both in vacuo and in solution. These charges, as well as the electron configuration of the cobalt atom in both isomers, are reported in Table 3. Taking as reference the two bare fragments $[Co(NH_3)_5]^{3+}$ and NO_2^-, the charge transferred from NO_2^- to pentaamminecobalt is 0.61 $|e^-|$ in the nitro isomer and 0.49 $|e^-|$ in the nitrito complex. The Co charges are +0.96 $|e^-|$ and +1.03 $|e^-|$ in the nitro and nitrito isomers, respectively. As mentioned above, the solvent increases the charge separation in the complex, significantly reducing the charge transferred from the nitro group to the Co complex: 0.46 $|e^-|$ in $[Co(NH_3)_5NO_2]^{2+}$ and 0.38 $|e^-|$ in $[Co(NH_3)_5ONO]^{2+}$. At same time, the NPA charges of the cobalt atom slightly increases to +0.98 $|e^-|$ and +1.04 $|e^-|$, respectively.

Finally, it must be pointed out that while the Co 3d population varies between the two isomers (from 7.70 to 7.64 $|e^-|$, for the nitro and nitrito complex in the gas phase, respectively), the Co 4s population remains essentially constant (about 0.30 $|e^-|$).

The slow nitrito → nitro linkage isomerization can be easily monitored by IR spectroscopy. The nitrite group shows two vibrational bands: the first is centered at about 1440 cm^{-1}, corresponding to an asymmetric NO_2 stretching, while the second is around 825 cm^{-1}, and has been assigned to the Co−NO_2 deformation.[12] The best diagnostic regions are at 1315 cm^{-1} for the nitro isomer (symmetric NO_2 stretching) and at 1065 cm^{-1} for the nitrito complex, where a strong band has been assigned to Co−ONO stretching vibration. This last band has been used to monitor the linkage isomerization: on aging a sample of $[Co(NH_3)_5ONO]^{2+}$ it decreases in intensity until it disappears completely.[12]

In Table 4 are reported the B3LYP results, while in Figures 2 and 3 are plotted the theoretical IR spectra computed either in the gas phase or in aqueous solution and reproduced by associating a single Lorentzian function to each computed wavenumber, with a half-height width of 10 cm^{-1}. Even if a direct comparison between theoretical harmonic wavenumbers and experimental anharmonic values is misleading, the theoretical values can be used to support the experimental assignments. The spectra of the two isomers can be easily distinguished in two main regions: one characteristic of the NH_3 groups and one assigned to the NO_2 moiety. In the first region, the NH stretching computed in the range 3500−3300 cm^{-1} for both

TABLE 3: Natural Population Analysis for the Two Isomers of Nitropentaamminecobalt(III) and the Corresponding Transition State (TS), Computed Either in the Gas Phase or in Aqueous Solution, and the Charge for the NH_3 Group in the Trans Position, $(NH_3)_{trans}$, and the Average Values for the Equatorial NH_3 Groups, $(NH_3)_{Eq}$

	gas phase		solution[a]		solution	
atom	charge	conformation	charge	conformation	charge	conformation
$[Co(NH_3)_5NO_2]^{2+}$						
Co	0.958	$4s^{0.30}\ 3d^{7.70}$	0.976	$4s^{0.30}\ 3d^{7.68}$	0.929	$4s^{0.30}\ 3d^{7.70}$
N1	0.292		0.305		0.292	
O2	−0.343		−0.422		−0.433	
O3	−0.343		−0.422		−0.433	
$(NH_3)_{trans}$	0.298		0.298		0.325	
$(NH_3)_{eq}$	0.249		0.316		0.330	
$[Co(NH_3)_5ONO]^{2+}$						
Co	1.027	$4s^{0.29}\ 3d^{7.64}$	1.044	$4s^{0.29}\ 3d^{7.62}$	1.000	$4s^{0.29}\ 3d^{7.66}$
N1	0.241		0.272		0.266	
O2	−0.603		−0.601		−0.553	
O3	−0.145		−0.290		−0.369	
$(NH_3)_{trans}$	0.262		0.306		0.330	
$(NH_3)_{eq}$	0.305		0.317		0.331	
TS						
Co	1.045	$4s^{0.30}\ 3d^{7.61}$	1.061	$4s^{0.30}\ 3d^{7.60}$	1.064	$4s^{0.30}\ 3d^{7.61}$
N1	0.202		0.204		0.188	
O2	−0.290		−0.414		−0.416	
O3	−0.512		−0.761		−0.576	
$(NH_3)_{trans}$	0.316		0.309		0.324	
$(NH_3)_{eq}$	0.293		0.423		0.354	

[a] Gas-phase geometry.

TABLE 4: Gas-Phase Harmonic Wavenumbers (cm^{-1}) Computed at the B3LYP/LANL2DZ Level[a]

$[Co(NH_3)_5NO_2]^{2+}$				$[Co(NH_3)_5ONO]^{2+}$			
gas phase	aqueous sol	exp.	assignment	gas phase	aqueous sol	exp	assignment
3554−3365	3456−3327	∼3200	NH stretch	3556−3370	3456−3364	∼3200	NH stretch
1683	1661	1595	NH_3 def	1684	1675	1595	NH_3 def
1466	1439	1440	NO_2 asym stretch	1586	1611	1460	ONO asym stretch
1257	1285	1315	NH_3 def + sym NO_2 stretch	1359	1353	1325	NH_3 def
877−834	900−803	850	NH_3 rock	846	899	1065	ONO sym stretch
757	777	825	NO_2 def	828−876	898−819	850	NH_3 rock
				718	791	825	NO_2 def

[a] Experimental data are from ref 12.

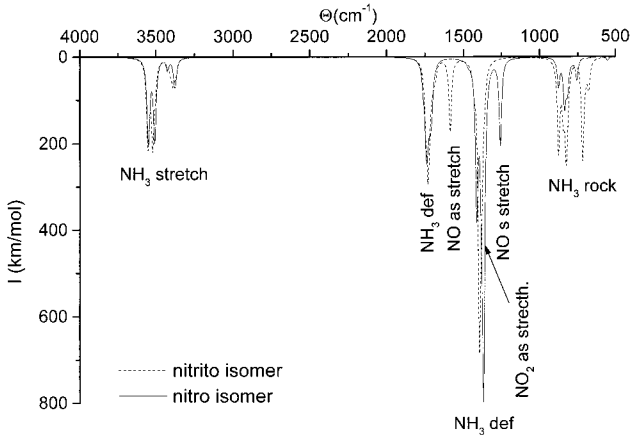

Figure 2. Theoretical IR spectra for the nitro and nitrito linkage isomers. The spectra are reproduced by associating a single Lorentzian function to each computed wavenumber, with a half-height width of 10 cm^{-1}.

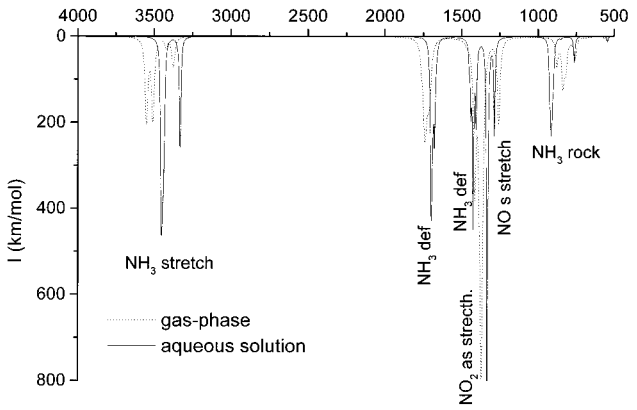

Figure 3. Theoretical IR spectra for the nitro isomer computed in gas phase (dotted line) and in aqueous solution (continuous line). The spectra are reproduced by associating a single Lorentzian function to each computed wavenumber, with a half-height width of 10 cm^{-1}.

isomers corresponds to the experimental bands around 3200 cm^{-1}. In a similar manner, the NH_3 deformation is predicted to be 1683 cm^{-1}, quite close to the experimental finding (1595 cm^{-1}). Finally, the NH_3 rocking mode, which is observed at around 850 cm^{-1} in both isomers, is calculated at 877 cm^{-1}. As concerns the NO_2 modes, they are well reproduced for the nitro isomer, the greatest error being 70 cm^{-1} for the symmetric stretching mode (1257 vs 1315 cm^{-1}, see Table 4). Greater errors (≈100 cm^{-1}) are found for the nitrito isomers. In particular, the highest NO stretching vibration is overestimated (1586 vs 1460 cm^{-1}), while the second is underestimated (846 vs 1065 cm^{-1}) with respect to the experimental values.

The plot of Figure 2 well evidenced the fingerprint regions of the two isomers: the NO_2 asymmetric stretching at 1257 cm^{-1} (experiment 1315 cm^{-1}) for the nitro complex and the ONO asymmetric stretching at 1586 cm^{-1} (experiment 1460 cm^{-1}) for the nitrito isomer.

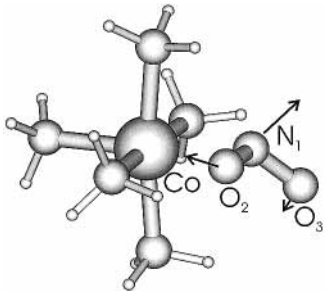

Figure 4. Structure of the transition state for the nitrito → nitro interconversion in the gas phase. The arrows on the picture indicate the different components of the transition vector ($\nu = 441i$ cm^{-1}).

As expected, in going from the gas phase to the aqueous solution, a significant shift toward lower frequencies is observed for all the vibrational modes, which reflects the variations of the geometrical parameters. This shift generally improves the agreement with the experimental wavenumbers, as can be seen from the data collected in Table 4. In particular, the greatest variations are found for the stretching modes of the ammonia ligands in the nitro isomer, while smaller shifts are computed for the modes of the nitrito group. In this last case, the modes of the nitrito isomer corresponding to the ONO symmetric stretch and to the NO_2 deformation increase +53 and +73 cm^{-1}, respectively.

The overall trend is reported in Figure 3, where the IR spectra of the nitro complex in the gas phase and in aqueous solution are plotted.

As mentioned in the Introduction, there is still a great ambiguity about the nature of the transition state (TS), the experimental data fitting two possible molecular rearrangement (structures I and III of Scheme 1). We have found a transition state along the path connecting the two linkage isomers, and its geometrical parameters are reported in Table 1. This molecular structure has been obtained by a full geometrical optimization, and has been characterized as a first-order saddle point, with one imaginary frequency ($\nu = 441i$ cm^{-1}). In Figure 4, we have reported the optimized structure of this TS, together with the transition vector components. As it appears from this sketch, this structure can be described as a heptacoordinate rearrangement, with the NO_2 moiety in a η_2 coordination. This was the only stationary point localized on the reaction path joining the two minima: all the other efforts to localize different TS structures led to one of the minimum energy structures, thus discharging all the other alternatives (structures II and III of Scheme 1). The geometrical parameters indicate that the N atom and one of the O atoms of the nitro ligand are at almost the same distance from the Co atom (2.38 vs 2.41 Å, respectively).

TABLE 5: Endothermicity (ΔE) and Activation Energy ($\Delta E^{\#}$) for the Linkage Isomerization Reaction of Nitritopentaamminecobalt(III) → Nitropentaamminecobalt(III)[a]

	B3LYP								
	gas phase		THF	acetone	water		exp		
	LANL2 DZ	LANL2 DZp	LANL2 DZ	LANL2 DZ	LANL2 DZ	LANL2 DZp	THF[b]	water[c]	solid state[d]
ΔE	1.0	4.7	1.7 (2.9)	2.4 (3.7)	3.3 (5.4)	7.3			
$\Delta E^{\#}$	30.1	34.3	(30.2)	(28.3)	21.7 (23.1)	25.8	25.3 ± 1.4	22.7 ± 0.2	22−26

[a] All values are in kcal/mol and refer to fully optimized geometries. In parentheses are reported the energies computed in solution using gas-phase geometries. [b] Reference 17. [c] Reference 4. [d] From ref 4.

All the other geometrical parameters, as those of the ammino ligands, are intermediate between the nitro and the nitrito isomer.

A better understanding of the electronic structure of the TS comes from an analysis of the NPA charges, reported in Table 3. The NO_2^- fragment has an overall charge of -0.6 $|e^-|$, thus suggesting that less charge (0.4 $|e^-|$) is transferred to the pentaammine complex than in the two minima. At the same time, the Co charge is greater (+1.05). These results indicate a molecular rearrangement with a Co−NO_2 bond with a partial ionic character.

Starting from the gas-phase structure, we have fully optimized the transition state in water. The obtained geometrical parameters are reported in Table 2. Also, this structure has been characterized as a first-order saddle point with one imaginary frequency ($\nu = 385i$ cm^{-1}). The overall geometrical rearrangement is similar to that found in vacuo, but some significant variations in the geometrical parameters can be observed. Among others, the Co−N1 and Co−O2 bond lengths are significantly longer (+0.1 Å) than in the gas phase. As it concerns all the other geometrical parameters, they follow the trends already observed for the nitrito isomer in going from gas phase to solution. The charge separation effect induced by the solvent is well evident in the NPA charges (see Table 3). In particular, the nitro ligand bears a charge of -0.80 $|e^-|$ in the fully relaxed structure; i.e., the charge transferred from the nitro group is reduced to 0.20 $|e^-|$.

The structures of the reactants and of the TS allow for the evaluation of a significant thermodynamic activation parameter, namely the activation volume ($\Delta V^{\ddagger}$). This quantity is certainly interesting in defining the nature of a substitution reaction, i.e., if the mechanism is dissociative, D, associative, A, intermediate associative, I_a, or intermediate dissociative, I_d. In this isomerization both A and D mechanisms are ruled out by experiments which suggest an intramolecular reaction.[10,11] The experimental work of Mares et al.[13] on the kinetics of isomerization of $[Co(NH_3)_5ONO]^{2+}$ reports a small and negative activation volume (-6.4 cm^3/mol) for the isomerization suggesting an I_a mechanism. In order to compute the activation volume we decided to evaluate the volume of the reactant and TS as proportional to the sum of all metal to donor atom distances as already applied in the literature for other substitution reaction.[52] The activation volume is therefore proportional to Σ, the difference between the TS and the $[Co(NH_3)_5ONO]^{2+}$ volumes estimated in such a way:

$$\Sigma = \sum_i d(\mathrm{M{-}X}_i)_{\mathrm{TS}} - d(\mathrm{M{-}X}_i)_{\mathrm{CoONO}}$$

where M is the cobalt atom and X (X = O, N) are the atoms of the nitrite moiety. From the computed structures, we find a $\Sigma_{vacuo} = -0.64$ Å and $\Sigma_{water} = -0.10$ Å. These values show a trend in agreement with the experimental findings,[13] further supporting an I_a mechanism.

In summary, our results confirm the type intermediate envisaged by Basolo and Pearson (I in Scheme 1),[11] and seem to rule out a η_3 rearrangement of the transition state (structure III in Scheme 1), originally suggested by Jackson and coworkers.[17]

TABLE 6: Different Contributions to the Free Energy of Solvation in Water (kcal/mol)[a]

	ΔG_{cav}	ΔG_{dis}	ΔG_{rep}	ΔG_{elet}	ΔG_{tot}
$[Co(NH_3)_5NO_2]^{2+}$	20.8	−22.7	5.3	−212.5,	−209.2
$[Co(NH_3)_5ONO]^{2+}$	21.1	−23.4	5.7	−208.2	−204.7
TS	21.1	−22.9	5.5	−217.4	−213.9

[a] See text for the definitions of the different terms. All the values have been computed using gas-phase geometries.

3.2. Thermodynamics and Kinetics of the Linkage Isomerization. It is well-known that the nitro isomer is strongly favored in any kind of solvent (>95%) or in the solid state,[17] while no data are available in the gas phase. Also, the activation energy for the nitrite/nitro interconversion have been evaluated in solution and it ranges between 19 and 26 kcal/mol, depending on the kind of solvent used.[4,13,17]

Our gas phase results are collected in Table 5. They indicate that the nitro isomer is only marginally more stable than the nitrito complex, the energy difference being 1.0 kcal/mol. The consideration of the extended basis set significantly stabilizes the nitro isomer over the nitrito one (+4.7 kcal/mol, see Table 5). Our final estimation, including ZPE corrections evaluated at the B3LYP/LANL2DZ level (+0.8 kcal/mol), is that the nitro is more stable than the nitrite of 3.9 kcal/mol.

A further stabilization of the nitro isomer is found in solution, which depends on the considered solvent. So, the nitro isomer is 1.7 kcal/mol more stable than the nitrito complex in THF, but the energy gap increases to 2.4 kcal/mol in acetone and 3.3 kcal/mol in water (fully relaxed geometries). Unfortunately, there are not direct measurements of the endothermicity, but these results are in agreement with the experimental evidences that the nitro isomer is more stable than the nitrito complex in solution.

But, why is the nitro isomer more stable in solution than the nitrito one? In the frame of a PCM approach, like the one considered here, it is possible to distinguish between different contributions to the total solvation free energy ΔG_{sol}:[27]

$$\Delta G_{sol} = \Delta G_{cav} + \Delta G_{dis-rep} + \Delta G_{elect}$$

where ΔG_{elect} is the electrostatic term, ΔG_{cav} is related to the work needed to form the molecular cavity in the solvent, and $G_{dis-rep}$ is related to the dispersion−repulsion interactions. These terms for $[Co(NH_3)_5NO_2]^{2+}$, $[Co(NH_3)_5ONO]^{2+}$, and TS are reported in Table 6. Our computations show that the nonelectrostatic contribution, i.e., the first two terms of the total solvation energy, is almost equal for the two isomers, being 3.4 and 3.3 kcal/mol for the nitro and nitrito complex, respectively. This contribution, as well as the others here discussed, have been evaluated freezing the molecular geometries at the gas-phase values. In contrast, the electrostatic term

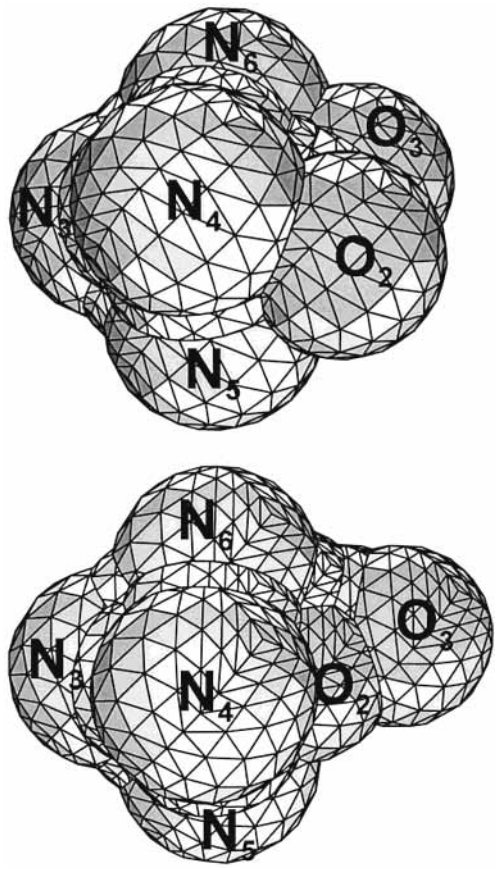

Figure 5. UATM cavities for the nitro (left) and nitrito complex. Atom labeling is the same as Figure 1.

is −212.5 kcal/mol for the nitro isomer and −208.2 kcal/mol for the nitrito complex. This difference arises from the different exposition to the solvent of the NO_2^- group in the two molecules as can been seen from the sketch of the two cavities reported in Figure 5. The further relaxation of the molecular geometry in solution decreases the energy gap to 3.3 kcal/mol in water.

In Table 5 is also reported the B3LYP activation energies for the isomerization reaction, both in the gas phase and in different solvents. The theoretical estimate suggests a very high barrier in the gas phase (30.1 kcal/mol at the B3LYP/LANL2DZ level), but this value is drastically reduced in solution. In fact, the barrier is 23.1 kcal/mol in water, using the gas-phase geometries. This significant difference in going from the gas phase to the solution (−7.0 kcal/mol) is, once again, due to the electrostatic interactions. In fact, the interactions between the solute and the solvent reaction field give an electrostatic contribution of −217.4 kcal/mol to the solvation energy, greater than that found for the two isomers, since the NO_2^- moiety is even more exposed in the TS. A small further reduction of the barrier (−2.4 kcal/mol) is obtained by relaxation of the geometries in water solution, so that our final estimate for the activation energy in water (including the basis set effect) is 25.8 kcal/mol. This value is close to the experimental estimate of 22.7 ± 0.2 kcal/mol,[4] thus showing the quality of our approach.

4. Conclusion

In the present paper, we report a comprehensive study on the thermodynamic and the kinetic of the linkage isomerization of nitrito pentaammine Co(III) in nitro pentaammine Co(III). Our results suggests that the nitro isomer is slightly favored in the gas phase with respect to the nitrito one. In contrast, bulk solvent effects strongly affect the equilibrium in favor of the nitro species. While these results are coherent with the experimental data, we have, for the first time, shown the nature of the transition state. In fact, we have found that the transition state of the nitrito/nitro interconversion can be described as a η_2-coordinated structure in the gas phase, quite high in energy. The solvent, strongly favoring a species with charge separation, increases the ionic character of the $Co-NO_2$ bond and, at the same time, decreases the activation energy of the reaction.

As last significant remark we want add a small comment about the interplay of theory and experiments. In particular, modern computational tools, even if developed for the study of organic systems, have now reached a sufficient level of reliability to allow their routine application to the study of complex inorganic systems. This paves the route for a better understanding of the subtle effects ruling many organometallic reactions, both in the gas phase and in condensed phase.

Acknowledgment. The authors thank prof. V. Barone (Naples, Italy) for fruitful discussions and helpful comments.

References and Notes

(1) Gibbs, W.; Genth, F. A. *Am. J. Sci.* **1857**, *24*, 86.
(2) Jørgensen, S. M. *Z. Anorg. Chem.* **1893**, *5*, 169.
(3) Kauffman, G. B. *Coord. Chem. Rev.* **1973**, *11*, 161, and reference therein.
(4) Basolo, F.; Pearson, R. G. *Mechanism of Inorganic Reactions*; Wiley: New York, 1967.
(5) Purcell K. F.; Kotz, J. C. *Inorganic Chemistry*; Holt Saunders: London, 1985.
(6) Jackson, W. G.; Cortez, S. *Inorg. Chem.* **1994**, *33*, 1921.
(7) Angus, P. M.; Jackson, W. G. *Inorg. Chem.* **1994**, *33*, 477.
(8) Jackson, W. G.; Sargeson, A. M. In *Rearrangements in Ground and Excited States*; de Mayo, P., Ed.; Academic Press: New York, 1980.
(9) Kapanadze, T. Sh.; Tsintsadze, G. V.; Kokunov, Y. V.; Buslaev, Y. A. *Polyhedron* **1990**, *9*, 1379
(10) Murmann, R. K.; Taube, H. *J. Am. Chem. Soc.* **1956**, *78*, 4886.
(11) Pearson, R. G., Henry, P. M.; Bergman, J. G.; Basolo, F. *J. Am. Chem. Soc.* **1954**, *76*, 5920.
(12) Penland, R. B.; Lane, T. J.; Quagliano, J. V. *J. Am. Chem. Soc.* **1956**, *78*, 887.
(13) Mares, M.; Palmer, D. A.; Kelm, H. *Inorg. Chim. Acta* **1978**, *27*, 153.
(14) Grenthe, I.; Nordin, E. *Inorg. Chem.* **1979**, *18*, 1869.
(15) Jackson, W. G.; Lawrance, G. A.; Lay, P. A.; Sargeson, A. M. *Inorg. Chem.* **1980**, *19*, 904.
(16) Rindermann, W.; Van Eldik, R.; Kelm, H. *Inorg. Chim. Acta* **1982**, *61*, 173.
(17) Jackson, W. G.; Lawrance, G. A.; Lay, P. A.; Sargeson, A. M. *Aust. J. Chem.* **1982**, *35*, 1561.
(18) Adamo, C.; di Matteo, A.; Barone, V. *Adv. Quantum Chem.* **1999**, *36*, 45.
(19) Ziegler, T. *Chem. Rev.* **1991**, *91*, 651.
(20) Becke, A. D. *J. Chem. Phys.* **1993**, *98*, 1372.
(21) Barone, V.; Adamo,C. *J. Phys. Chem.* **1996**, *100*, 2094.
(22) Adamo, C.; Barone, V.; Bencini, A.; Totti, F.; Ciofini, I. *Inorg. Chem.* **1999**, *38*, 1996.
(23) Bauschlicher, C. W.; Ricca, A.; Partridge, H.; Langhoff, S. In *Recent Advances in Density Functional Thoery;* Chong, D. P., Ed.; World Scientific Publishing Co.: Singapore, 1997.
(24) Siegbahn, P. E. M. *J. Am. Chem. Soc.* **1996**, *118*, 1487.
(25) Musaev, D. G.; Svensson, M.; Morokuma, K.; Strömberg, S.; Zetterberg, K.; Siegbahn, P. E. M. *Organometallics* **1997**, *16*, 1933.
(26) Holthausen, M. C.; Heineman, C.; Cornehl, H. H.; Koch, W.; Schwarz, H. *J. Chem. Phys.* **1995**, *102*, 4931.
(27) Tomasi, J., Persico, M. *Chem. Rev.* **1994**, *94*, 2027.
(28) Rega, N.; Cossi, M.; Barone, V. *J. Am. Chem. Soc.* **1997**, *119*, 12962.
(29) Cossi, M.; Adamo, C.; Barone, V. *Chem. Phys. Lett.* **1998**, *297*, 1.
(30) Pomelli, C. S.; Tomasi, J.; Sola, M. *Organometallics* **1998**, *17*, 3164.
(31) Rotzinger, F. P.; Benoit, M. *Inorg. Chem.* **2000**, *39*, 944.
(32) Frisch, M. J.; Trucks, G. W.; Schlegel, H. B.; Scuseria, G. E.; Stratmann, R. E.; Burant, J. C.; Dapprich, S.; Millam, J. M.; Daniels, A.

D.; Kudin, K. N., Strain, M. C.; Farkas, O.; Tomasi, J.; Barone, V.; Cossi, M.; Cammi, R.; Mennucci, B.; Pomelli, C.; Adamo C.; Clifford, S.; Ochterschi, J.; Cui, Q.; Gill, P. M. W.; Johnson, B. G.; Robb, M. A.; Cheeseman, J. R.; Keith, T.; Petersson, Morokuma, K.; Malick, D. K.; Rabuck, A. D.; G. A.; Montgomery, J. A.; Raghavachari, K.; Al-Laham, M. A.; Zakrewski, V. G.; Ortiz, J. V.; Foresman, J. B.; Cioslowski, J.; Stefanov, B. B.; Nanayakkara, A.; Liu, J.; Liashenklo, A.; Piskorz, P.; Komaromi, I.; Challacombe, M.; Peng, C. Y.; Ayala, P. Y.; Chen, W.; Wong, M. W.; Andres, J. L.; Replogle, E. S.; Gomperts, R.; Martin, R. L.; Fox, D. J.; Binkley, J. S.; DeFrees, D. J.; Baker, J.; Stewart, J. P.; Head-Gordon, M.; Gonzalez, C.; Pople. J. A. *Gaussian 99* (Revision B.5)+; Gaussian Inc.: Pittsburgh, PA, 2000.

(33) Frisch, Æ.; Frisch, M. J. *Gaussian 98 User's Reference*; Gaussian, Inc.: Pittsburgh, PA, 1998.

(34) Becke, A. D. *Phys. Rev. B* **1988**, *38*, 3098.

(35) Lee, C.; Yang, W.; Parr, R. G. *Phys. Rev. B* **1988**, *37*, 785.

(36) Hay, P. J.; Wadt, W. R. *J. Chem. Phys.* **1985**, *82*, 299.

(37) Dunning, T. M. *J. Chem. Phys*. **1971**, *55*, 716. Dunning, T. M. *J. Chem. Phys*. **1970**, *53*, 2823

(38) Hay, P. J. *J. Phys. Chem.* **1996**, *100*, 5.

(39) Blomberg, M. R. A.; Siegbahn, P. E. In *Transition State Modeling for Catalysis*; ACS Symposium Series 721; Truhlar, D. G., Morokuma, K., Eds.; American Chemical Society: Washington, DC, 1999; p 49.

(40) Giju, K. T.; Bickelhaupt, F. M.; Frenking, G. *Inorg. Chem.* **2000**, *39*, 4776.

(41) Cossi, M.; Barone, V.; Cammi, R.; Tomasi, J. *Chem. Phys. Lett.* **1996**, *255*, 327.

(42) Barone, V.; Cossi, M.; Tomasi, J. *J. Chem. Phys.* **1997**, *107*, 3210.

(43) Barone, V.; Cossi, M.; Tomasi, J. *J. Comput.Chem*. **1998**, *19*, 407.

(44) Barone, V.; Cossi, M. *J. Phys. Chem. A* **1998**, *102*, 1995.

(45) Rega, N.; Cossi, M.; Barone, V. *J. Chem. Phys*. **1998**, 109, 11060

(46) Cossi, M.; Barone, V. *J. Chem. Phys*. **1998**, 109, 6246

(47) Reed, A.E.; Curtiss, L.A.; Weinhold, F. *Chem. Rev*., **1988**, *88*, 899.

(48) *NBO 4.0 program*; Glendening, E. D.; Badenhoop, J. K.; Reed, A. E.; Carpenter, J. E.; Weinhold, F. Theoretical Chemistry Institute, University of Wisconsin, Madison, WI, 1996.

(49) *Molden* release 3.4; CAOS/CAMM Center, The Netherlands, 1998.

(50) Cotton, F. A.; Edwards, W. T. *Acta Crystallogr. B* **1968**, *24*, 474.

(51) Halpern, J.; Palmer, R. A.; Blakely, L. M. *J. Am. Chem. Soc*. **1966**, *88*, 2877.

(52) Rotzinger, F. *J. Am. Chem. Soc*. **1996**, *118*, 6760.